

Substitution reactions of dichlorobis(betadiketonato-*O,O'*) titanium(IV) complexes with aryl diolato ligands: An experimental and computational study



Kathrin H. Hopmann^{a,b}, Annemarie Kuhn^c, Jeanet Conradie^{a,c,*}

^a Center for Theoretical and Computational Chemistry (CTCC), University of Tromsø, N-9037 Tromsø, Norway

^b Department of Chemistry, University of Tromsø, N-9037 Tromsø, Norway

^c Department of Chemistry, University of the Free State, 9300 Bloemfontein, South Africa

ARTICLE INFO

Article history:

Received 19 June 2013

Accepted 11 September 2013

Available online 23 September 2013

Keywords:

Titanium
Substitution
Kinetics
DFT
Mechanism

ABSTRACT

Substitution reactions of complexes $\text{Ti}(\beta\text{-diketonato})_2\text{Cl}_2$, in which the two monodentate Cl^- ligands are replaced by different bidentate aryl-diolato ligands (catechol, naphthol, biphenol, binaphthol, or methylenebinaphthol), produce remarkably hydrolytically stable titanium(IV) complexes with 5-, 7- or 8-membered chelating rings. The lability of the chlorine ligand in the parent compound is dependent on the strength of the electron donating properties of the spectator β -diketonato ligand around the titanium centre. The reactivity of $\text{Ti}(\text{RCOCHCOR}')_2\text{Cl}_2$ complexes according to the β -diketonato ligand $(\text{RCOCHCOR}')^-$ follows the order $(\text{PhCOCHCOPh})^- > (\text{PhCOCHCOCH}_3)^- > (\text{CH}_3\text{COCHCOCH}_3)^-$, in line with results for other known transition metal complexes. Detailed substitution kinetics along with the X-ray crystal structure of a mono-chloride $\text{Ti}(\beta\text{-diketonato})_2(\text{Cl})(\text{naphthol})$ reaction intermediate are reported. DFT calculations on the reaction of $\text{Ti}(\text{acac})_2\text{Cl}_2$ with different aryl-diolato ligands reveal that chlorine substitution proceeds via a two-step interchange mechanism with the formation of two seven-coordinated transition states and one six-coordinated intermediate. The computed mechanism agrees very well with experimental kinetic and X-ray data.

© 2013 Elsevier Ltd. All rights reserved.

1. Introduction

The mechanistic behaviour of titanium(IV) complexes is of fundamental interest because of their wide spread use as catalysts in different organic reactions [1] and in medical applications in anti-cancer therapy [2]. The origin of the tremendous catalytic activity of titanium(IV) catalysts is the high Lewis acidity or electron deficiency, which can be easily tuned by variations on the electronic properties of the ligands, but the down fall is its high sensitivity to hydrolysis. Titanium alkoxy systems, for example, are effective catalysts in a variety of processes, but the sensitivity to hydrolysis results in some Ti–OR bond cleavage when exposed to water that is produced as a by-product in the reaction (esterification reactions [3]). Studies have shown that the resistance towards hydrolysis can be increased by introducing bulky³ or chelating electron-rich oxygen-based ligands [4]. A very successful series of enantioselective catalysts, based on chelating binaphtholate ligand (BINOL), is widely employed [5].

The $\text{Ti}(\beta\text{-diketonato})_2\text{Cl}_2$ complex and related compounds are good models for studying ligand substitution because only the chloride coordinated ligand is labile. The bidentate β -diketonato ligand enhances the stability of the 12-electron mononuclear *cis*- $\text{Ti}(\beta\text{-diketonato})_2\text{Cl}_2$ complex through ligand $p_\pi \rightarrow \text{metal } d_\pi$ donation. Each β -diketonato ligand has one π -donor orbital which interacts with an empty Ti d-orbital in this π -electron bonding [6].

In this paper we have carried out kinetic and computational studies in order to extend our understanding of the mechanistic behaviour of titanium in substitution reactions. We describe the synthesis of a remarkably hydrolytically stable series of complexes containing three-electron-rich oxygen-based bidentate ligands: bis(acetylacetonato)-aryl-diolato-titanium(IV) complexes. The aryl-diolato-ligands form 5-, 7- and 8-membered chelating rings. Two complexes, the complex with 2,3-dihydroxynaphthalene, and an intermediate containing 2,3-dihydroxynaphthalene, are reported here for the first time. For the later, we report a crystal structure that corresponds to the mono-chloride intermediate of the substitution reaction. Computational studies on the formation of the a 5-, 7- or 8-membered $\text{Ti}(\text{acac})_2(\text{aryl-diolato})$ complex provide insight into the mechanistic details of the substitution reactions.

* Corresponding author at: Department of Chemistry, University of the Free State, 9300 Bloemfontein, South Africa. Tel.: +27 51 4012194; fax: +27 51 4446384.

E-mail address: conradj@ufs.ac.za (J. Conradie).

2. Experimental section

2.1. Materials and apparatus

Solid reagents used in preparations (Merck, Aldrich and Fluka) were used without further purification. Liquid reactants and solvents were distilled prior to use; water was doubly distilled. Organic solvents were dried according to published methods [7].

2.2. Synthesis

All operations were carried out under anhydrous conditions in a dry N₂ atmosphere. All glassware was flame-dried and was allowed to cool in a stream of dry N₂. The N₂ atmosphere was maintained throughout the reaction. Filtrations and recrystallisations were performed under a blanket of N₂. All solvents were dried and distilled under N₂ immediately before use. Complex numbering is according to Scheme 1.

2.2.1. Dichlorobis(β-diketonato-O,O')titanium(IV), **1a–1c** (Ti(β-diketonato)₂Cl₂)

The Ti(β-diketonato)₂Cl₂ complexes were synthesized according to published methods [8,9] as described for Ti(acac)₂Cl₂ **1a**, Ti(ba)₂Cl₂ **1b** and Ti(dbm)₂Cl₂ **1c**, with acac = acetylacetonato = (CH₃-COCHCOCH₃)⁻, ba = benzoylacetonato = (PhCOCHCOCH₃)⁻, dbm = dibenzoylmethanato = (PhCOCHCOPh)⁻ and Ph = C₆H₅.

2.2.2. Bis(acetylacetonato-O,O')(1,2-benzenediolato-O,O')titanium(IV), **2** (Ti(acac)₂cat) and bis(acetylacetonato-O,O')(2,2'-binaphthyldiolato-O,O')titanium(IV), **5** (Ti(acac)₂binaph)

To a stirred solution of 1 mmol dihydroxy-aryl ligand (either 1,2-dihydroxybenzene or 2,2'-dihydroxybinaphthyl) in dichloro-

methane (3 ml), dichlorobis(acetylacetonato-O,O')titanium(IV), Ti(acac)₂Cl₂, (0.431 g/1 mmol) in dichloromethane (2 ml) was syringed dropwise at room temperature with an immediate colour change. The reaction mixture instantly turned dark red and the dihydroxy-aryl ligand dissolved on shaking. After standing 5 h at room temperature, the reaction mixture was layered with hexane (7 ml) and allowed to stand for 2 days. The precipitate was isolated by filtration and washed with hexane and recrystallized from dichloromethane/*n*-hexane.

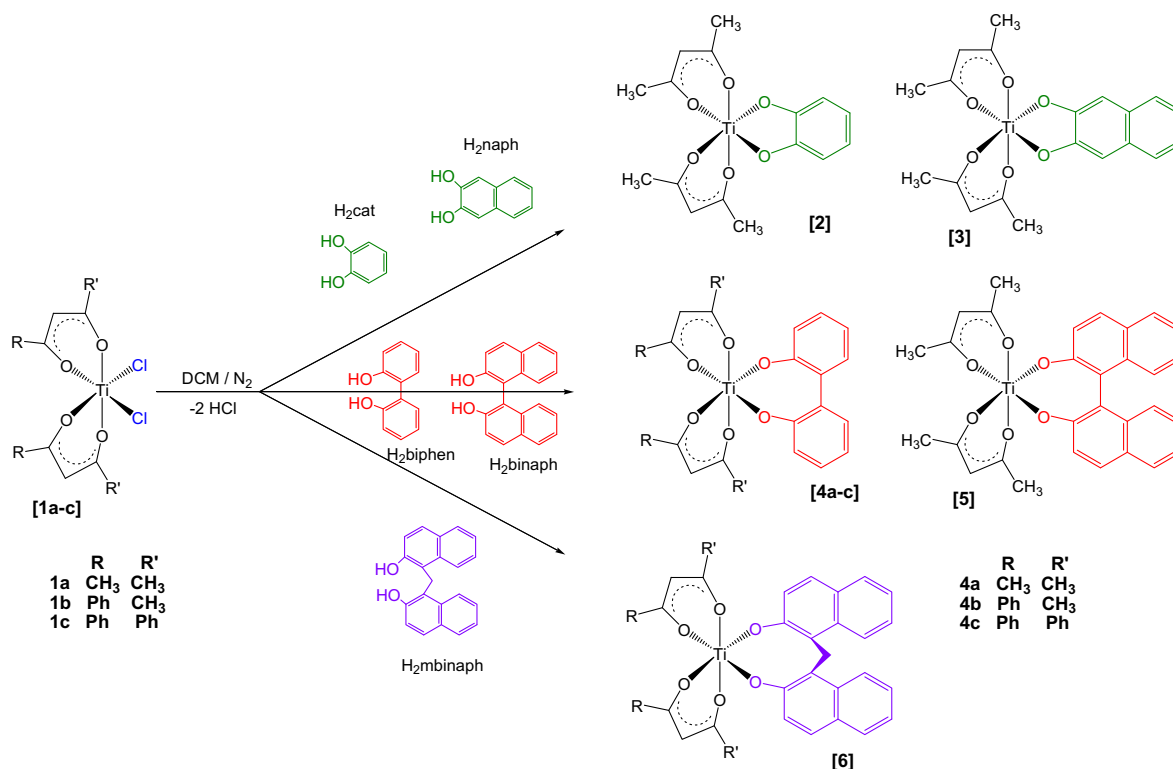
2.2.2.1. *Ti(acac)₂cat* **2**. Yield 12% (0.043). M.p. > 200 °C. Colour: red/brown. ¹H NMR (300 MHz, δ/ppm, CDCl₃): 2.20 (s, 12H, 4 × CH₃), 5.90 (s, 2H, 2 × CH), 6.28 (m, 2H, catH), 6.65 (m, 2H, catH). Elemental Anal. Calc. for TiC₁₆H₁₈O₆: C, 61.2; H, 5.8. Found: C, 61.0; H, 5.9%.

2.2.2.2. *Ti(acac)₂binaph* **5**. Yield 60% (0.311). M.p. > 200 °C. Colour: red/brown. ¹H NMR (600 MHz, δ/ppm, CDCl₃): 2.00 (s_{br}, 12H, 4 × CH₃), 5.77 (s, 2H, 2 × CH), 7.12 (t, 2H, binaphH), 7.25 (t, 2H, binaphH), 7.27 (d, 2H, binaphH), 7.34 (d, 2H, binaphH), 7.83 (d, 4H, binaphH). Elemental Anal. Calc. for TiC₃₀H₂₆O₆: C, 73.5; H, 5.3. Found: C, 73.7; H, 5.4%.

2.2.3. Bis(acetylacetonato-O,O')(2,3-naphthalenediolato-O,O')titanium(IV), **3** (Ti(acac)₂naph)

A 10 times excess of 2,3-dihydroxynaphthalene (H₂naph) was added to Ti(acac)₂(Cl)₂ in dichloromethane, stirred for 2 h. After standing 5 h at room temperature, the reaction mixture was layered with hexane (7 ml) and allowed to stand for 2 days. The precipitate was isolated by filtration and washed with hexane and recrystallized from dichloromethane/*n*-hexane.

M.p. > 200 °C. Colour: red/brown. ¹H NMR (300 MHz, δ/ppm, CDCl₃): 2.16 (s, 12H, 4 × CH₃), 5.90 (s, 2H, 2 × CH), 6.64 (s, ¹H,



Scheme 1. Synthesis of Ti(β-diketonato)₂(L) complexes with L = cat **2**, naph **3**, biphen **4a**, binaph **5** and mbinaph **6** with H₂cat = 1,2-dihydroxybenzene or catechol; H₂naph = 2,3-dihydroxynaphthalene or naphthol; H₂biphen = 2,2'-dihydroxybiphenyl or biphenol; H₂binaph = 2,2'-dihydroxybinaphthyl or binaphthol; H₂mbinaph = 1,1'-dihydroxy-methylene-binaphthyl or methylenebinaphthol. β-diketones; Hacac = 2,4-pentanedione = CH₃COCH₂COCH₃, for **1a**, **2**, **3**, **4a**, **5** and **6**; Hba = 1-phenyl-1,3-butanedione = PhCOCH₂COCH₃ for **1b** and **4b** and Hdbm = 1,3-diphenyl-1,3-propanedione PhCOCH₂COPh for **1c** and **4c**.

naphH), 7.18 (dd, 2H, naphH), 7.54 (dd, 2H, naphH). Elemental Anal. Calc. for $\text{TiC}_{20}\text{H}_{20}\text{O}_6$: C, 66.0; H, 5.5. Found: C, 66.1; H, 5.5%.

2.2.4. Bis(β -diketonato-*O,O'*)(2,2'-biphenyldiolato-*O,O'*)titanium(IV), **4a–4c** ($\text{Ti}(\beta\text{-diketonato})_2(\text{biphen})$)

The $\text{Ti}(\beta\text{-diketonato})_2(\text{biphen})$ complexes were synthesized according to published methods [10,11] as described for $\text{Ti}(\text{acac})_2$ (biphen) **4a**, $\text{Ti}(\text{ba})_2(\text{biphen})$ **4b** and $\text{Ti}(\text{dbm})_2(\text{biphen})$ **4c**.

2.2.5. Bis(acetylacetonato-*O,O'*)(1,1'-methylenebinaphthyldiolato-*O,O'*)titanium(IV), **6** ($\text{Ti}(\text{acac})_2(\text{mbinaph})$)

To a stirred solution of 2,2'-dihydroxy-methylene-binaphthyl (0.300 g, 1 mmol) in CH_3CN (15 ml), dichlorobis(acetylacetonato-*O,O'*)titanium(IV), $\text{Ti}(\text{acac})_2\text{Cl}_2$ (1.0 mmol) in CH_3CN (5 ml) was syringed in dropwise at room temperature with an immediate colour change (clear/grey to red). The reaction mixture was stirred and purged with a slow stream of N_2 (to evolve the hydrogen chloride gas) for 20 min and then refluxed for 4–6 h. The reaction mixture was cooled to room temperature and the solvent evaporated to dryness. The product was obtained in two ways (i) the residue was redissolved in CH_3CN and allowed to crystallise out or (ii) the residue was recrystallized from dichloromethane/*n*-hexane.

Yield 62% (0.3368 g). M.p. > 200 °C. Colour: red. ^1H NMR (300 MHz, δ/ppm , CDCl_3): 2.07 (s, 12H, 4 \times CH_3), 4.79, 5.16 (br, ^1H each, CH_2), 5.80 (s, 2H, 2 \times CH), 7.01 (br, 2H, mbinaphH), 7.27 (br, 2H, mbinaphH), 7.40 (br, 2H, mbinaphH), 7.54 (d, 2H, mbinaphH), 7.73 (d, 1H, mbinaphH), 8.36 (br, 2H, mbinaphH). Elemental Anal. Calc. for $\text{TiC}_{31}\text{H}_{28}\text{O}_6$: C, 73.8; H, 5.6. Found: C, 73.7; H, 5.5%.

2.2.6. Chlorobis(acetylacetonato-*O,O'*)(3-hydroxy-2-naphtholato-*O,O'*)titanium(IV), **7** ($\text{Ti}(\text{acac})_2(\text{Cl})(\text{Hnaph})$)

The synthetic route of **2** and **5** was followed, using 2,3-dihydroxynaphthalene (H_2naph) as ligand. The product obtained was a mixture of **3** and **7**. A crystal of **7** suitable for X-ray studies was isolated from the solution. The NMR of the crystal of **7** also yielded a mixture of **3** and **7**.

M.p. > 200 °C. Colour: red/brown. ^1H NMR (300 MHz, δ/ppm , CDCl_3): 2.01–2.31 (br, 12H, 4 \times CH_3), 5.89 (s, 2H, 2 \times CH), 7.25 (s, 1H, naphH), 7.27 (t, 1H, naphH), 7.31 (t, 1H, naphH), 7.34 (s, 1H, naphH), 7.63 (d, 1H, naphH), 7.64 (d, 1H, naphH), 7.75 (br, 1H, OH).

2.3. Spectroscopy and spectrophotometry

NMR measurements at 25 °C were recorded on a Bruker Avance II 600 NMR spectrometer [^1H (600.130 MHz)]. The chemical shifts were reported relative to SiMe_4 (0.00 ppm). Positive values indicate downfield shift. UV–Vis spectra were recorded on a Cary 50 Probe UV–Vis spectrophotometer.

2.4. Kinetic measurements

The substitution reaction was monitored on the UV–Vis (by monitoring the change in absorbance at the 380 nm for complex **1b** and at 450 nm for **1c**) spectrophotometers. All kinetic measurements were monitored under pseudo-first-order conditions with $[\text{H}_2\text{biphen}]$ 10 to 200 times the concentration of the $\text{Ti}(\beta\text{-diketonato})_2\text{Cl}_2$ complex in CH_3CN solution. The concentration $\text{Ti}(\beta\text{-diketonato})_2\text{Cl}_2 \cong 0.0002 \text{ mol dm}^{-3}$. Kinetic measurements, under pseudo-first-order conditions for different concentrations of $\text{Ti}(\beta\text{-diketonato})_2\text{Cl}_2$ at a constant $[\text{H}_2\text{biphen}]$, confirmed that the concentration of $\text{Ti}(\beta\text{-diketonato})_2\text{Cl}_2$ did not influence the value of the observed kinetic rate constant. A linear relationship between UV absorbance, A , and concentration, C , confirmed the validity of the Beer Lambert law ($A = \epsilon Cl$ with $l = \text{path length} = 1 \text{ cm}$) for the complexes **1a** and **4a** at experimental wave lengths $\lambda_{\text{max}} = 340 \text{ nm}$

($\epsilon/\text{dm}^3\text{mol}^{-1}\text{cm}^{-1}$ is 1830(20) for **1a** and 4890(30) for **4a**). The observed first-order rate constants were obtained from least-square fits of absorbance vs. time data [12].

2.5. Calculations

Pseudo-first-order rate constants, k_{obs} , were calculated by fitting kinetic data [12] to the first-order equation [13] $[A]_t = [A]_0 e^{(-k_{\text{obs}} t)}$ with $[A]_t$ and $[A]_0$ the absorbance of the indicated species at time t and at $t = 0$ (UV–Vis). The experimentally determined pseudo first order rate constants were converted to second order rate constants, k_1 (for the first reaction step), by determining the slope of the linear plots of k_{obs} against the concentration of the incoming biphenolato ligand. Non-zero intercepts implied that $k_{\text{obs}} = k_1[\text{biphen}] + k_s$ and that the first order rate constant for a solvent pathway, k_s , in the proposed reaction mechanism exists. The first order rate constant for the second reaction step will be denoted by k_2 . All kinetic mathematical fits were done utilizing the fitting program MINSQ [12]. The error of all the data are presented according to crystallographic conventions, for example $k_{\text{obs}} = 0.0236(1) \text{ s}^{-1}$ implies $k_{\text{obs}} = (0.0236 \pm 0.0001) \text{ s}^{-1}$. The activation parameters were determined from the Eyring relationship [13] and the activation free energy $\Delta G^\ddagger = \Delta H^\ddagger - T\Delta S^\ddagger$.

2.6. Computational methods

Calculations of the reaction pathways were performed with the B3LYP functional as implemented in the GAUSSIAN 03 package [14]. Geometries were optimized in gas phase with a triple- ζ basis set, 6-311G(d,p). Solvation effects were computed by performing single-point calculations on the optimized geometries with the IEFPCM model, using CH_3CN as solvent and a dielectric constant of 36.64. Thermochemical quantities were calculated from frequency calculations at the same level of theory as optimizations. The frequency calculations were also employed to confirm the nature of the obtained stationary points, which exhibited only positive eigenvalues for minima and one imaginary frequency for transition states.

2.7. X-ray crystal structure determination

Crystals of $\text{Ti}(\text{acac})_2(\text{Cl})(\text{Hnaph})$ **7** were obtained from recrystallization in chloroform. The crystal of **7** was mounted on a glass fiber and used for the X-ray crystallographic analysis. The X-ray intensity data were measured on a Bruker X8 Apex II 4K CCD diffractometer area detector system equipped with a graphite monochromator and Mo $K\alpha$ fine-focus sealed tube ($\lambda = 0.71073 \text{ \AA}$) operated at 1.5 KW power (50 kV, 30 mA). The detector was placed at a distance of 3.75 cm from the crystal. Crystal temperature during the data collection was kept constant at 100(2) K using an Oxford 700 series cryostream cooler.

The initial unit cell and data collection were achieved by the APEX2 software [15] utilizing COSMO [16] for optimum collection of more than a hemisphere of reciprocal space. A total of 1709 frames were collected with a 0.5° scan width in φ and ω . An exposure time of 90 s frame $^{-1}$ was used. The frames were integrated using a narrow-frame integration algorithm and reduced with the SAINT-Plus [17] and XPREP [17] software packages respectively. The integration of the data using a triclinic cell yielded a total of 18989 reflections to a maximum θ angle of 28.33° , of which 4996 were independent with a $R_{\text{int}} = 0.0365$. Analysis of the data showed no significant decay during the data collection. Data were corrected for absorption effects using the multi-scan technique SADABS [18] with minimum and maximum transmission coefficients of 0.9543 and 0.8663 respectively. The structure was solved by the direct methods package SIR97 [19] and refined using the WINGX software

package [20] incorporating SHELXL [21]. The final anisotropic full-matrix least-squares refinement on F^2 with 258 parameters converged at $R1 = 0.0348$ for the observed data and $wR2 = 0.0871$ for all data. The GOF was 1.064. The largest peak on the final difference electron density synthesis was $0.49 \text{ e } \text{Å}^{-3}$ at 0.67 Å from O4 and the deepest hole $-0.31 \text{ e } \text{Å}^{-3}$ at 0.67 Å from Ti1.

The aromatic, methylene, methyl and hydroxyl H atoms were placed in geometrically idealized positions ($C/O-H = 0.84-0.98 \text{ Å}$) and constrained to ride on their parent atoms with $U_{iso}(H) = 1.2U_{eq}(C)$ for aromatic, methylene and $U_{iso}(H) = 1.5U_{eq}(C/O)$ for methyl and hydroxyl. The methyl and hydroxyl H's were located from a Fourier difference map and refined with ideal geometries. Non-hydrogen atoms were refined with anisotropic displacement parameters. Atomic scattering factors were taken from the International Tables for Crystallography Volume C [22]. The molecular plot was drawn using the DIAMOND program [23] with a 50% thermal envelope probability for non-hydrogen atoms. Hydrogen atoms were drawn as arbitrary sized spheres with radius of 0.135 Å .

3. Results and discussion

3.1. Synthesis of bis(acetylacetonato-*O,O'*)(aryl diolato-*O,O'*) Ti(IV) complexes

The series of $Ti(acac)_2L$ complexes with $L = \text{cat } \mathbf{2}$, naph $\mathbf{3}$, biphen $\mathbf{4a}$, binaph $\mathbf{5}$, mbinaph $\mathbf{6}$, was synthesised according to Scheme 1. The structures and names of the investigated complexes are summarised in Scheme 1. The complexes $\mathbf{2}$ [24] $\mathbf{4a}$ [10] $\mathbf{5}$ [25] and $\mathbf{6}$ [26] have been reported previously, while complex $\mathbf{3}$ is reported here for the first time. The reaction, initiated by adding $Ti(acac)_2Cl_2$, $\mathbf{1a}$ (see Section 3.2.1. for the synthesis of $\mathbf{1a}$), to the poorly dissolved ligand in dichloromethane, changes colour immediately to dark red in all cases. These aryl-diolato ligands, which are slightly soluble in dichloromethane at room temperature, dissolve rapidly (as the reaction proceeds) on shaking. After standing 5 h at room temperature, the mixture is layered with hexane and allowed to stand for 2 days, before the red crystalline product is isolated by filtration and washed with hexane.

Complexes $\mathbf{1a-c}$ are extremely moisture sensitive and hydrolyze easily forming the fine white powder TiO_2 [27], whereas complexes $\mathbf{2-6}$ exhibit a high hydrolytic stability (no precipitate was observed when dissolved in 0.01% water/ CH_3CN within 6 weeks) and are "air stable" for more than 3 years. The strong electron donation to the titanium centre from the aryl diolato ligand's oxygens relative to the electron withdrawing Cl^- -ions, may contribute to the enhanced hydrolytic stability.

Complexes in this series form 5-, 7- and 8-membered chelated rings while keeping the acac ligands constant. The chemical shifts of the methine proton of the acac-ligand in the coordinate complex and for the uncoordinated Hacac (included for comparison) are listed in Table 1. The acac methine proton of $Ti(acac)_2L$ complexes $\mathbf{2-6}$ ($\delta = 5.77-5.90 \text{ ppm}$) is slightly upfield shifted relative to the parent complex $Ti(acac)_2Cl_2$ ($\delta = 6.00 \text{ ppm}$) $\mathbf{1}$. This is expected

Table 1
 1H NMR chemical shifts for the methine protons of complexes $\mathbf{1-6}$.

No	Compound	Ring size	$^1H/ppm$ methine H
–	Hacac	–	5.50
$\mathbf{1a}$	$Ti(acac)_2Cl_2$	–	6.00
$\mathbf{2}$	$Ti(acac)_2cat$	5	5.90
$\mathbf{3}$	$Ti(acac)_2naph$	5	5.90
$\mathbf{4a}$	$Ti(acac)_2biphen$	7	5.79
$\mathbf{5}$	$Ti(acac)_2binaph$	7	5.77
$\mathbf{6}$	$Ti(acac)_2mbinaph$	8	5.82

since the aryl-diolato ligands are more electron-donating than Cl^- . The size of the chelated aryl-diolato ring (5-, 7- and 8-membered chelated rings) or the addition of an extra phenyl ring on the aryl-diolato ligand has only a very slight effect on the shift of the acac methine proton.

The aryl-diolato ring protons of the chelated complex are shifted slightly upfield relative to the uncoordinated ligand. In contrast, the resonance for the chelated β -diketonato ligand is always shifted downfield relative to the uncoordinated β -diketone (in the studied complexes); electric field effects and pi bonding could contribute to the downfield shifts [28].

3.2. The $Ti(\beta\text{-diketonato})_2Cl_2 + H_2biphen$ reaction

In the following section we discuss in detail the parent complexes $Ti(\beta\text{-diketonato})_2Cl_2$ (β -diketonato = acac [10], ba and dbm, $\mathbf{1a-c}$) and the kinetics and the product complexes $\mathbf{4a-c}$ of the reaction of $\mathbf{1a-c}$ with $H_2biphen$, involving replacement of the two monodentate Cl^- ligands by one bidentate biphen. Under second order conditions, the related reaction, $Ti(\beta\text{-diketonato})_2Cl_2 + H_2naph$ reaction yielded a mixture of $\mathbf{3}$ and the mono-chloride complex $\mathbf{7}$ ($Ti(\beta\text{-diketonato})_2(Cl)(Hnaph)$) as products. $\mathbf{7}$ was successfully crystallized, see Section 3.3.

3.2.1. The reactants

The reactant complexes $Ti(acac)_2Cl_2$ $\mathbf{1a}$, $Ti(ba)_2Cl_2$ $\mathbf{1b}$ and $Ti(dbm)_2Cl_2$ $\mathbf{1c}$ were prepared by treating $TiCl_4$ with two equivalents of the appropriate β -diketone, isolated and purified by recrystallisation before use [8,9]. Complexes $\mathbf{1a-c}$ are extremely moisture and oxygen sensitive but are stable if sealed and stored under Argon, at room temperature. If exposed to atmospheric oxygen and water vapour, the complex converts to a fine, white powder, titanium dioxide (TiO_2), consistent with the complete hydrolysis and decomposition, proposed by Keppler and Heim [27]. The $Ti(\beta\text{-diketonato})_2Cl_2$ complexes adopt *cis* configurations with Cl in the *cis* position (as opposed to the *trans* configurations where Cl is in the *trans* position). This allows for the bidentate β -diketonato ligand to enhance the stability of the 12-electron $Ti(\beta\text{-diketonato})_2Cl_2$ complex through ligand \rightarrow metal π -electron donation [6]. Complex $\mathbf{1b}$, containing unsymmetrical β -diketonato ligands, exists as three distinct *cis* geometrical isomers see Fig. 1, while $\mathbf{1a}$ and $\mathbf{1c}$, with symmetrical β -diketonato ligands, exist as a single *cis* conformer. This is in agreement with NMR data, force field [29] and DFT calculations [11]. Variable-temperature NMR data further indicated that in solution the three *cis* isomers of $\mathbf{1b}$ exist in a fast equilibrium with *cis-trans-cis* as the major isomer [11] which is the same isomer that was characterized by single crystal X-ray data [30]. The geometry of all of the reactant complexes in the solid state are known from crystal X-ray studies, viz. $\mathbf{1a}$ [31], $\mathbf{1b}$ [30] and $\mathbf{1c}$ [32].

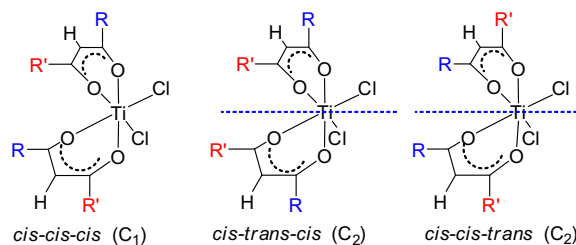


Fig. 1. The stereochemistry of *cis*- $Ti(\beta\text{-diketonato})_2Cl_2$ complexes (position according to Cl , R and R'): *cis-cis-cis* isomer (point group C_1), *cis-cis-trans* (point group C_2) and *cis-trans-cis* (point group C_2). The rotation axis, where applicable, is indicated with a dotted blue line. (For interpretation of the references to colour in this figure legend, the reader is referred to the web version of this article.)

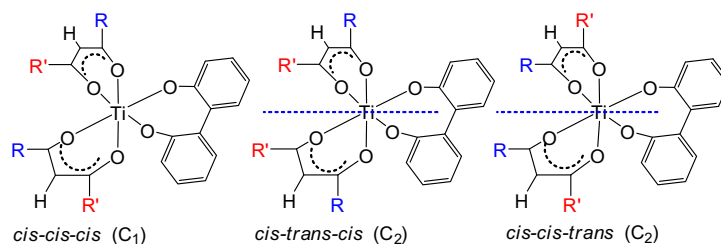


Fig. 2. The stereochemistry of $\text{Ti}(\beta\text{-diketonato})_2\text{biphen}$ complexes (position according to O_{biphen} , R and R'): *cis-cis-cis* isomer (point group C_1), *cis-cis-trans* (point group C_2) and *cis-trans-cis* (point group C_2). The rotation axis, where applicable, is indicated with a dotted blue line. (For interpretation of the references to colour in this figure legend, the reader is referred to the web version of this article.)

3.2.2. The products

The bis(β -diketonato) (biphenyldiolato)titanium(IV) product complexes $\text{Ti}(\text{acac})_2(\text{biphen})$ **4a**, $\text{Ti}(\text{ba})_2(\text{biphen})$ **4b** and $\text{Ti}(\text{dbm})_2(\text{biphen})$ **4c** were obtained by the substitution of two monodentate Cl^- ligands in $\text{Ti}(\beta\text{-diketonato})_2\text{Cl}_2$ for the bidentate biphen. The $\text{Ti}(\beta\text{-diketonato})_2\text{biphen}$ complexes **4a–4c** adopt one or more of three possible *cis* configurations, with the bidentate biphen O atoms in *cis* positions, see Fig. 2. Similar to the reactants, complexes (**4b**) containing unsymmetrical β -diketonato ligands, exist as three distinct *cis* geometrical isomers whereas **4a** and **4c**, with symmetrical β -diketonato ligands, exist as a single *cis* conformer. Variable temperature NMR studies and DFT calculations [11] showed the *cis-trans-cis* isomer of **4b** to be the main isomer in solution, the same isomer that was isolated and characterized by X-ray crystallography [11]. The geometries of $\text{Ti}(\text{acac})_2(\text{biphen})$ **4a** [10] and $\text{Ti}(\text{ba})_2(\text{biphen})$ **4b** [11] are known from single crystal X-ray data.

3.2.3. Experimental substitution kinetics

The substitution of the two monodentate Cl^- ligands for bidentate H_2biphen in $\text{Ti}(\beta\text{-diketonato})_2\text{Cl}_2$ complexes **1a–1c**, was followed on the UV–Vis spectrophotometer. Two reaction steps were observed, a relatively fast first step (with a half-life of 1–20 min depending on the reactant and $[\text{H}_2\text{biphen}]$) and a second step *c.a.* 10 times slower than the first reaction step. The rate constants of the two steps were determined independently. The results obtained are in agreement with those obtained by Burgess et al. [33]; each step involves the replacement of a chloride ion, with rate-limiting ring closure occurring in the second step. Since the reaction was followed under pseudo first order conditions with H_2biphen in excess, first-order kinetics in $[\text{H}_2\text{biphen}]$ was observed for the first step, the first reaction being second order overall with a rate constant $k_1 = k_{\text{obs}}/[\text{H}_2\text{biphen}]$. The second step was $[\text{H}_2\text{biphen}]$ independent, *i.e.* first order with rate constant k_2 . Rate constants for the first (k_1) and second (k_2) stages of substitution of $\text{Ti}(\beta\text{-diketonato})_2\text{Cl}_2$

complexes **1a–1c** are given in Table 2 and the results plotted as a function of the incoming H_2biphen concentration in Fig. 3. The non-zero intercept of these graphs, implies that the solvent, CH_3CN , contributes to the reaction mechanism, although only in a relatively minor way. The results obtained are thus consistent with a reaction scheme (Scheme 2) with two kinetically distinct steps (including also a solvent pathway), yet the exact coordination nature of the reaction intermediate (*i.e.* associative, dissociative or interchange mechanism) requires elucidation.

The general rate law applicable to the first $[\text{H}_2\text{biphen}]$ dependent step is given by $\text{Rate} = k_{\text{obs}}[\text{Ti}(\beta\text{-diketonato})_2\text{Cl}_2]$ [34,35] with the pseudo-first-order rate constant $k_{\text{obs}} = k_5 + k_1[\text{H}_2\text{biphen}]$ and k_1 the second-order rate constant for the first step of the substitution process, k_2 the first-order rate constant for the second step of the substitution process and k_5 the first order rate constant for a solvent pathway.

The activation parameters, the entropy of activation, ΔS^\ddagger , and activation enthalpy, ΔH^\ddagger , determined from a temperature dependence study, is also given in Table 2. The large negative activation entropy obtained suggests that the substitution process proceeds *via* an associative or interchange mechanism. The structural changeover from six- to seven-coordinate is possible since the 12-electron (d^0) $\text{Ti}(\beta\text{-diketonato})_2\text{Cl}_2$ species is coordinatively unsaturated. A 5-coordinated cationic species, $[\text{Ti}(\text{acac})_2\text{Cl}]^+$, formed by breaking the first Ti–Cl bond (in a dissociative mechanism), is considerably less likely. Stable Ti(IV) complexes with coordination numbers greater than six, for example, 7- and 8-coordination, are known [36,37]. From the experimental observations, it is not possible to determine the structure of the reaction intermediate.

From the experimental rate constants, it is observed that the reactivity of $\text{Ti}(\text{R}(\text{COCHCOR}')_2)_2\text{Cl}_2$ complexes towards ligand substitution follows the order $\text{Ti}(\text{PhCOCHCOPh})_2\text{Cl}_2 > \text{Ti}(\text{PhCOCHC}(\text{OCH}_3)_2)_2\text{Cl}_2 > \text{Ti}(\text{CH}_3\text{COCHCOCH}_3)_2\text{Cl}_2$. This is the same trend of reactivity reported for various transition metal β -diketonato complexes containing the same β -diketonato ligands [38].

Table 2

Kinetic data and activation parameters for the substitution of biphen for the two monodentate Cl^- ligands $\text{Ti}(\beta\text{-diketonato})_2\text{Cl}_2$ in CH_3CN as solvent, and the ADF/PW91 calculated HOMO energy (E_{HOMO}) of **1a–1c**.

T ($^\circ\text{C}$)	k_1 ($\text{dm}^3\text{mol}^{-1}\text{s}^{-1}$)	k_5 (s^{-1})	k_2 (s^{-1})	ΔH^\ddagger (kJ mol^{-1})	ΔS^\ddagger ($\text{J mol}^{-1}\text{K}^{-1}$)	ΔG^\ddagger (kJ mol^{-1})	Reference
Ti(acac)₂Cl₂ 1a							
15.0	0.062(2)	0.00012(3)					[10]
25.0	0.153(4)	0.00461(7)	0.0015(2)	59.6	−60.8	77.7	
36.2	0.365(5)	0.0133(1)					
Ti(ba)₂Cl₂ 1b							
10.0	0.141(4)	0.0004(1)					This study
25.0	0.331(9)	0.0028(3)	0.0009(2)	36.0(6)	−133(2)	76(1)	
40.0	0.691(2)	0.0082(3)					
Ti(dbm)₂Cl₂ 1c							
9.5	0.1439(6)	0.00055(9)					This study
25.5	0.485(9)	0.0029(2)	0.0003(1)	52.6(8)	−79(1)	76(1)	
40.0	1.35(4)	0.0097(5)					

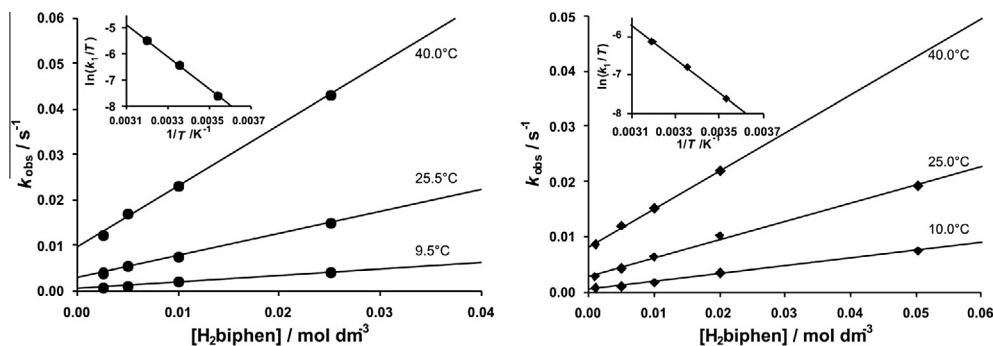
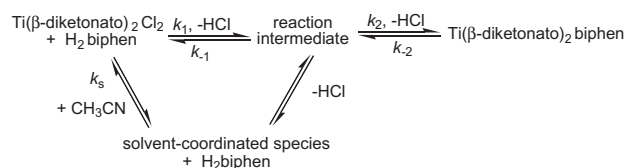


Fig. 3. Temperature and H_2biphen concentration dependence of the first reaction step of the substitution of biphen for the two monodentate Cl^- ligands in $\text{Ti}(\beta\text{-diketonato})_2\text{Cl}_2$ in CH_3CN , $\beta\text{-diketonato} = \text{ba} = (\text{PhCOCHCOCH}_3)^-$ (left) and $\text{dbm} = (\text{PhCOCHCOPh})^-$ (right), $[\text{Ti complex}] = 0.1 \text{ mmol dm}^{-3}$. Inset: Linear dependence between $\ln(k_1/T)$ and $1/T$, as predicted by the Eyring equation (k_1 is the second order rate constant for the first reaction step).



Scheme 2. Proposed scheme showing both the direct and solvent pathways.

3.3. Crystal structure of $\text{Ti}(\text{acac})_2(\text{Cl})(\text{Hnaph})$ **7**

Under second order conditions, the $\text{Ti}(\text{acac})_2\text{Cl}_2 + \text{H}_2\text{naph}$ reaction yielded a mixture of $\text{Ti}(\text{acac})_2(\text{Cl})(\text{Hnaph})$ (**7**) and the aryl-diolato complex $\text{Ti}(\text{acac})_2(\text{naph})$ (**3**) as products. Complex **7** was successfully crystallized, revealing that it is formed from the $\text{Ti}(\text{acac})_2\text{Cl}_2$ parent compound (**1a**) through substitution of a single chloride ligand. The mono-chloride complex could correspond to an intermediate in the substitution reaction resulting in formation of the aryl-diolato complex (**3**) from **1a**. This is confirmed by theoretical studies (*vide infra*). A molecular diagram showing the numbering scheme of **7** is presented in Fig. 4. Crystal data and details for data collections and refinements are summarized in Table S1 of the Supplementary data.

Molecule **7** crystallized on general positions with the central Ti ion showing severe distortions in its octahedral coordination environment. These distortions are due to both steric and electronic effects. To exemplify this observation, the expected three perpendicular axis of the ideal coordination environment are bent (Cl1-Ti1-O1 , O4-Ti1-O2 and O3-Ti1-O5 are $174.35(4)$, 170.39 and $172.37(5)^\circ$ respectively), possibly to accommodate the chelation of the acac molecules. The strong hydrogen bonding interaction

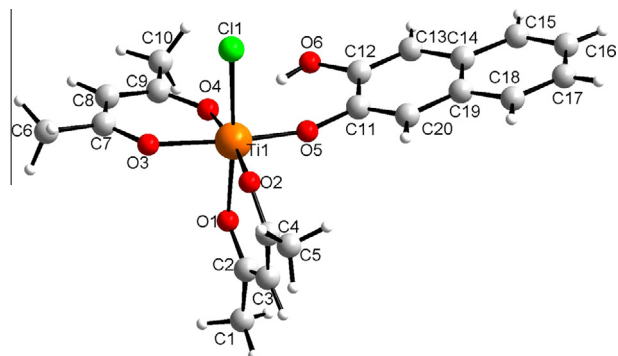


Fig. 4. The molecular structure (30% probability displacement ellipsoids) of $\text{Ti}(\text{acac})_2(\text{Cl})(\text{Hnaph})$, **7**, showing the numbering scheme.

Table 3
Hydrogen bonds for **7** [\AA and $^\circ$].

D-H...A	d(D-H)	d(H...A)	d(D...A)	<(DHA)
O(6)-H(6)...O(4)	0.84	1.95	2.7828(16)	169.4
C(5)-H(5A)...Cl(1)#1	0.98	2.85	3.8142(18)	169.4
C(8)-H(8)...Cl(1)#2	0.95	2.86	3.7425(17)	154.9
C(20)-H(20)...Cl(1)#1	0.95	2.78	3.6688(16)	155.4
C(3)-H(3)...O(6)#3	0.95	2.39	3.310(2)	162.9
C(16)-H(16)...Ct(1)#4	0.95	2.97	3.524(2)	118
C(5)-H(5C)...Ct(2)#1	0.98	2.82	3.595(2)	136
C(6)-H(6A)...Ct(3)#5	0.98	2.65	3.555(2)	153
C(10)-H(10C)...Ct(3)#6	0.98	2.51	3.458(2)	163

Symmetry transformations used to generate equivalent atoms: #1 $-x, -y+1, -z+2$ #2 $-x+1, -y+1, -z+1$ #3 $x-1, y, z$ #4 $x, y, z+1$ #5 $x, y, z-1$ #6 $x-1, -y, -z+2$.

(See Table 3) of the monodentate 2,3-naphthyldiol to a neighbouring O4 of one of the acac's is one of the reasons of the resulting orientation¹ and also attributes to the distortion coordination axis. The acac ligands are also not planar to their coordination planes ($9.087(3)^\circ$ ² and $8.93(7)^\circ$ ³). In addition the five coordinating oxygens have varying bond lengths, primarily ascribed to the induced *trans* effect. For the *trans* O2 and O4 atoms (both from acac ligands) the distances differ marginally ($1.9493(11)$ vs. $1.9876(11)$ \AA). The remaining two oxygens on the two acac's are even further weakened by the differing *trans* ligands. For O1 the chloride *trans* to it results in a Ti1-O1 distance of $2.0124(12)$ \AA and for O3 the strong bonding from the 2,3-naphthyldiol ($\text{Ti1-O5} = 1.7914(11)$ \AA) *trans* to it weakens the Ti1-O3 bond to $2.0009(12)$ \AA .

Despite the numerous aromatic rings in the complex, the only possible $\pi-\pi$ stackings in the crystal packing arrangement have slippage values of >3 \AA . Packing in the crystal is governed by $\text{C-H}\cdots\text{Cl/O}$ and $\text{C-H}\cdots\pi$ interactions (Fig. 5a). Of notice are the $\text{C-H}\cdots\pi$ interactions that generate dimeric units of the compound situated over inversion centres, whereas $\text{C-H}\cdots\text{O}$ and tri-furcated

¹ The 2,3-naphthyldiol is not parallel to the O2-O3-O4-O5 plane. Due to the twisted nature of the coordination environment the angle of $14.15(3)^\circ$ between these two planes should be used with caution (the fitted atoms of the O2-O3-O4-O5 plane has a rms deviation of 0.0775 whereas the fitted atoms of the 2,3-naphthyldiol has a rms = 0.0326).

² Angle take between planes formed by O1-Ti1-O2 and O1-C1-C2-C3-O2. Deviations of atoms in acac backbone from the plane: O1 = 0.0339(8) \AA , C1 = -0.0500(11) \AA , C2 = 0.0187(15) \AA , C3 = 0.0404(9) \AA and O2 = -0.0430(8) \AA . RMS deviation of fitted atoms = 0.0387 \AA .

³ Angle take between planes formed by O3-Ti1-O4 and O3-C7-C8-C9-O4. Deviations of atoms in acac backbone from the plane: O3 = 0.0057(7) \AA , C7 = -0.0093(11) \AA , C8 = 0.0066(11) \AA , C9 = -0.0007(11) \AA and O4 = -0.0023(7) \AA . RMS deviation of fitted atoms = 0.0058 \AA .

C–H...Cl link these together to be propagated along the *a* and *b* axis respectively, see Fig. 5b.

3.4. Computational study of the $\text{Ti}(\text{acac})_2\text{Cl}_2 + \text{aryl-diolato}$ reaction

3.4.1. Computational study of the $\text{Ti}(\text{acac})_2\text{Cl}_2 + \text{H}_2\text{biphen}$ reaction

DFT calculations [11] in agreement with crystal X-ray studies, show that the $\text{Ti}(\beta\text{-diketonato})_2\text{Cl}_2$ reactant **1a–1c** and the $\text{Ti}(\beta\text{-diketonato})_2(\text{biphen})$ product complexes **4a–4c** all adopt an octahedral geometry around the Ti centre. In addition to experiment, the quantum chemical approach makes it possible to calculate the energy and structure of transition states and reaction intermediates, not always observed experimentally. DFT calculations are here presented for the $\text{Ti}(\text{acac})_2\text{Cl}_2 + \text{H}_2\text{biphen}$ reaction to gain more insight into the structure of the transition states and possible reaction intermediates for formation of **4a** from **1a**.

The reactant structure ($\text{Reac}_{\text{biphen}}$) comprising $\text{Ti}(\text{acac})_2\text{Cl}_2$ and biphen is shown in Fig. 6a. From here the computed mechanism proceeds through two reaction steps as found experimentally. The optimized transition state of the first reaction step ($\text{TS1}_{\text{biphen}}$) indicates that attack of the hydroxyl oxygen on the Ti metal, dissociation of chloride and proton transfer from the attacking hydroxyl to the dissociating chloride ion can occur in a single step. The optimized $\text{TS1}_{\text{biphen}}$ structure displays a 7-coordinated pentagonal bipyramidal geometry. The attacking oxygen atom is positioned 2.14 Å from the Ti metal, whereas the scissile Ti–Cl bond is elongated to 3.17 Å (Fig. 6b), which is 0.85 Å longer than in the reactant complex (Fig. 6a). The proton of the attacking hydroxyl interacts strongly with the dissociating chloride ion with a Cl...H–O distance of 2.02 Å. Dissociation of the chloride ion is further facilitated by a hydrogen bonding interaction with the free hydroxyl group of the incoming ligand. Analysis of the transition state eigenvector shows dominating contributions from four bonds, the scissile Ti–Cl and O–H bonds and the forming Ti–O and Cl–H bonds, indicating that dissociation and formation of these bonds occurs concertedly. The computed imaginary frequency for TS1 is low, -73.96 cm^{-1} , which can be explained with the contribution of several heavy atoms to the reaction coordinate (given that the frequency is inversely proportional to the square root of the reduced mass of the involved nuclei) [39]. The computed activation enthalpy (including solvent effects and thermal corrections at 298.15 K) for TS1 is 60.8 kJ mol^{-1} (Table 4), in good agreement with the experimentally determined reaction enthalpy of 59.6 kJ mol^{-1} . Entropy contributions were also

computed, amounting to a value of $-46.7 \text{ J mol}^{-1} \text{ K}^{-1}$ (Table 4). Given that entropy calculations are very sensitive to low frequency modes, this value should be considered an estimation only. Nonetheless, it compares well with the experimentally obtained activation entropy of $-60.8 \text{ J mol}^{-1} \text{ K}^{-1}$. The computed activation Gibbs free energy ΔG^\ddagger is 74.7 kJ mol^{-1} , which is close to the experimentally determined value of 77.7 kJ mol^{-1} .

The intermediate geometry is six-coordinated and exhibits coordination of the biphenol molecule to the Ti through one oxygen atom ($\text{Inter}_{\text{biphen}}$, Fig. 6c). A stable 7-coordinated intermediate could not be obtained. The released HCl molecule is hydrogen-bonded to the free hydroxyl of biphenol. The computed ΔG value for the intermediate is $-12.2 \text{ kJ mol}^{-1}$. The estimated entropy is slightly positive and amounts to only $+4.0 \text{ J mol}^{-1} \text{ K}^{-1}$. The computed results for the first reaction step, involving a seven-coordinated transition state and a six-coordinated intermediate, indicate that the substitution reaction occurs through an interchange mechanism (as an associative mechanism would require formation of a 7-coordinated intermediate).

The second transition state ($\text{TS2}_{\text{biphen}}$) for attack of the second hydroxyl oxygen on the Ti centre is similar to the first transition state, exhibiting a 7-coordinated pentagonal bipyramidal geometry and involving concerted oxygen attack, chloride release and proton transfer (Fig. 6d). At the TS2 geometry, the attacking oxygen atom is positioned 2.24 Å from the Ti atom. The scissile Ti–Cl bond is elongated to 3.13 Å. The O–H bond of the attacking hydroxyl is slightly elongated from 0.98 Å at the intermediate to 1.03 Å at TS2. The Cl...H–O interaction is strong, with a distance of 1.83 Å. The computed activation enthalpy for the second step is 76.4 kJ mol^{-1} relative to the intermediate (65.4 kJ mol^{-1} relative to the reactant, Table 4). The computed activation Gibbs free energy ΔG^\ddagger is 91.9 kJ mol^{-1} relative to the intermediate (79.7 kJ mol^{-1} relative to the reactant, Table 4). These values agree well with experimental results, 77.7 and 89.1 kJ mol^{-1} for the two steps respectively, see Table 4, and also indicate that the second step of the reaction is slower than the first step.

The optimized product structure shows a six-coordinated Ti-complex (Fig. 6e). The two released HCl molecules are found hydrogen bonded to the complex. The computed reaction energy for the overall reaction is 10.0 kJ mol^{-1} , which indicates that the product is slightly less stable than the reactant. Removal of HCl, either by evaporation (during synthesis) or by diffusing away into solution (during reaction kinetics) drives the reaction to completion.

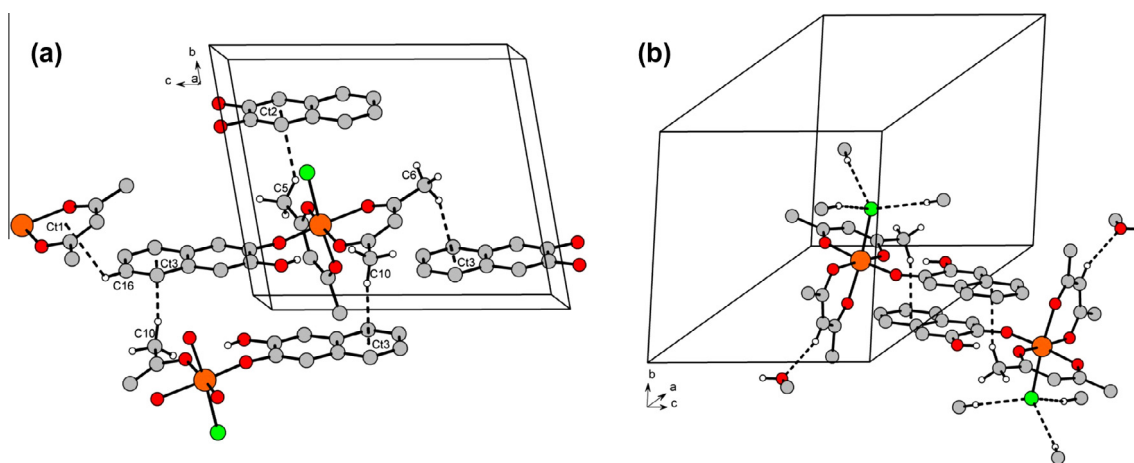


Fig. 5. (a) Packing diagram of **7** showing only C–H... π interactions. (b) Packing diagram of **7** showing the C–H...O and tri-furcated C–H...Cl interactions that link these units together along the *a* and *b* axis respectively. Hydrogen atoms not part of the interactions as well as parts of the neighbouring molecules have been omitted for clarity in this figure.

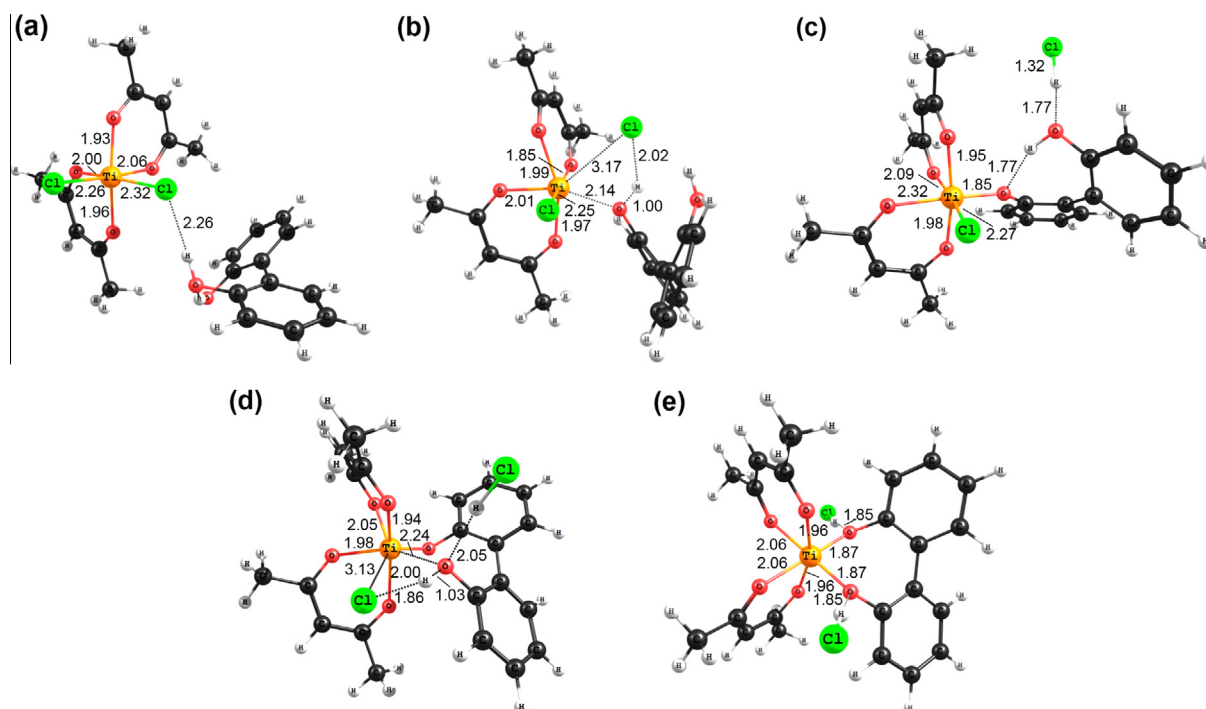


Fig. 6. DFT calculated optimized structures of the $\text{Ti}(\text{acac})_2\text{Cl}_2 + \text{H}_2\text{biphen}$ reaction (leading to formation of **4a**) with (a) ReaCbiphen , (b) $\text{TS1}_{\text{biphen}}$, (c) $\text{Inter}_{\text{biphen}}$, (d) $\text{TS2}_{\text{biphen}}$ and (e) $\text{Prod}_{\text{biphen}}$ (bonds breaking or forming are shown with dashed lines in the TS structures).

Table 4
Computed energies for biphenol substitution at $\text{Ti}(\text{acac})_2\text{Cl}_2$ (298.15 K).

$\text{Ti}(\beta)_2\text{Cl}_2$	Computed				Experimental		
	ΔH (kJ mol ⁻¹)	ΔS (J mol ⁻¹ K ⁻¹)	ΔG (kJ mol ⁻¹)	ΔG^\ddagger (kJ mol ⁻¹)	ΔH^\ddagger (kJ mol ⁻¹)	ΔS^\ddagger (J mol ⁻¹ K ⁻¹)	ΔG^\ddagger (kJ mol ⁻¹)
ReaCbiphen	0.0	0.0	0.0				
$\text{TS1}_{\text{biphen}}$	60.8	-46.7	74.7	74.7	59.6	-60.8	77.7
$\text{Inter}_{\text{biphen}}$	-11.0	4.0	-12.2				
$\text{TS2}_{\text{biphen}}$	65.4	-47.8	79.7	91.9			89.1
$\text{Prod}_{\text{biphen}}$	13.9	13.2	10.0				

Based on the DFT calculations, the proposed reaction pathway for the substitution reaction between $\text{Ti}(\beta\text{-diketonato})_2\text{Cl}_2$ and H_2biphen may thus be presented as in [Scheme 3](#) for $\beta\text{-diketonato} = \text{acac}$, where the first $[\text{H}_2\text{biphen}]$ dependent step is the formation of a 6-coordinated $[\text{Ti}(\beta\text{-diketonato})_2(\text{Cl})(\text{Hbiphen})]$ intermediate, and the second $[\text{H}_2\text{biphen}]$ independent step being rate-limiting ring closure. Both reaction steps involve simultaneous chloride dissociation and $\text{Ti}-\text{O}_{\text{naph}}$ bond formation, implying an overall interchange mechanism for this substitution reaction.

3.4.2. Computational study of the $\text{Ti}(\text{acac})_2\text{Cl}_2 + \text{H}_2\text{naph}$ reaction

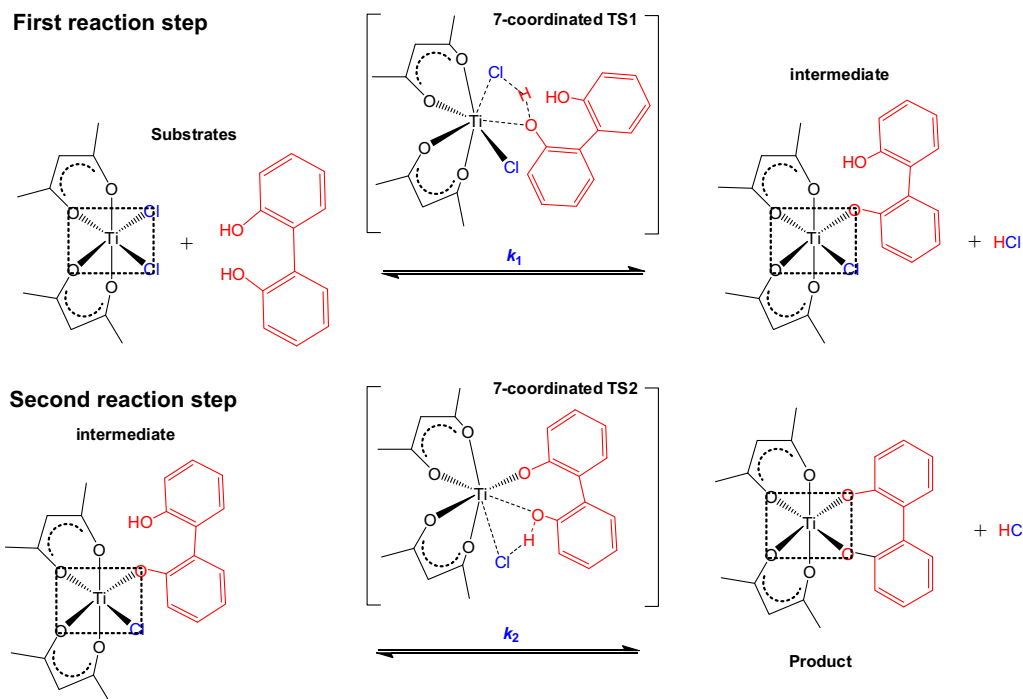
The X-ray crystal structure of **4a** containing a 7-membered aryl diolato ring [10] and **6** containing an 8 membered aryl diolato ring²⁶ were reported previously, while no structure of **2** or **3** containing a 5-membered aryl diolato ring is published to date. To provide more insight in the structure of a dichlorobis(betadiketonato-*O,O'*)titanium(IV) complex containing a 5-membered aryl diolato ring, and in order to compare to the results obtained above for **4a**, we also performed a theoretical study on the $\text{Ti}(\text{acac})_2\text{Cl}_2$ (**1a**) + H_2naph reaction leading to complex **3**.

The optimized geometry for the transition state of the first reaction step (TS1_{naph} , [Fig. 7](#)) shows that chloride substitution occurs in the same fashion as with biphenol above ([Fig. 6](#)). At TS1_{naph} , attack of one hydroxyl oxygen onto the Ti centre occurs simultaneously with chloride dissociation and abstraction of the hydroxyl proton

by chloride. The critical distances at TS1_{naph} are slightly different than with biphenol as substrate, showing that proton transfer to chloride has progressed somewhat further at TS1_{naph} (the $\text{Cl}\cdots\text{H}$ distance is 1.80 Å, [Fig. 7b](#)) than at $\text{TS1}_{\text{biphen}}$ ($\text{Cl}\cdots\text{H}$ is 2.02 Å, [Fig. 6b](#)). The computed energies show that the barrier for the first reaction step with H_2naph is 74.2 kJ mol⁻¹ ([Table 5](#)), which is essentially the same as for biphenol (74.7 kJ mol⁻¹, [Table 4](#)).

The six-coordinated intermediate geometry $\text{Inter}_{\text{naph}}$ ([Fig. 7c](#)) has a computed relative energy of 2.8 kJ mol⁻¹ ([Table 5](#)). Note that the crystallographically obtained structure of the monochloride complex **7** reported above ([Fig. 4](#)) corresponds to the complex $\text{Inter}_{\text{naph}}$ ([Fig. 7c](#)).⁴ The X-ray structure thus provides additional support for the proposed interchange substitution mechanism ([Scheme 3](#)). From the intermediate, the reaction progresses through the seven-coordinated TS2_{naph} ([Fig. 7d](#)), involving attack of the second hydroxyl oxygen on the Ti centre. At the optimized geometry of TS2_{naph} , the critical distances are similar to TS1_{naph} except for the $\text{Ti}\cdots\text{O}$ distance, which is somewhat shorter (2.02 Å at TS2_{naph}). The computed barrier for TS2_{naph} is 66.0 kJ mol⁻¹ ([Table 5](#)), which is lower than for TS1_{naph} . Thus the first step is rate-limiting for the reaction of $\text{Ti}(\text{acac})_2\text{Cl}_2$ and

⁴ The X-ray structure of **7** ([Fig. 3](#)) corresponds to the enantiomer of $\text{Inter}_{\text{naph}}$ ([Fig. 6c](#)). However, the mechanism for the reaction between the achiral H_2naph and **1a** will be the same for the two possible enantiomers of **1a**.



Scheme 3. Schematic presentation of the proposed interchange mechanism of the substitution reaction between $\text{Ti}(\text{acac})_2\text{Cl}_2$ (**1a**) and H_2biphen to afford $\text{Ti}(\text{acac})_2(\text{biphen})$ (**4a**).

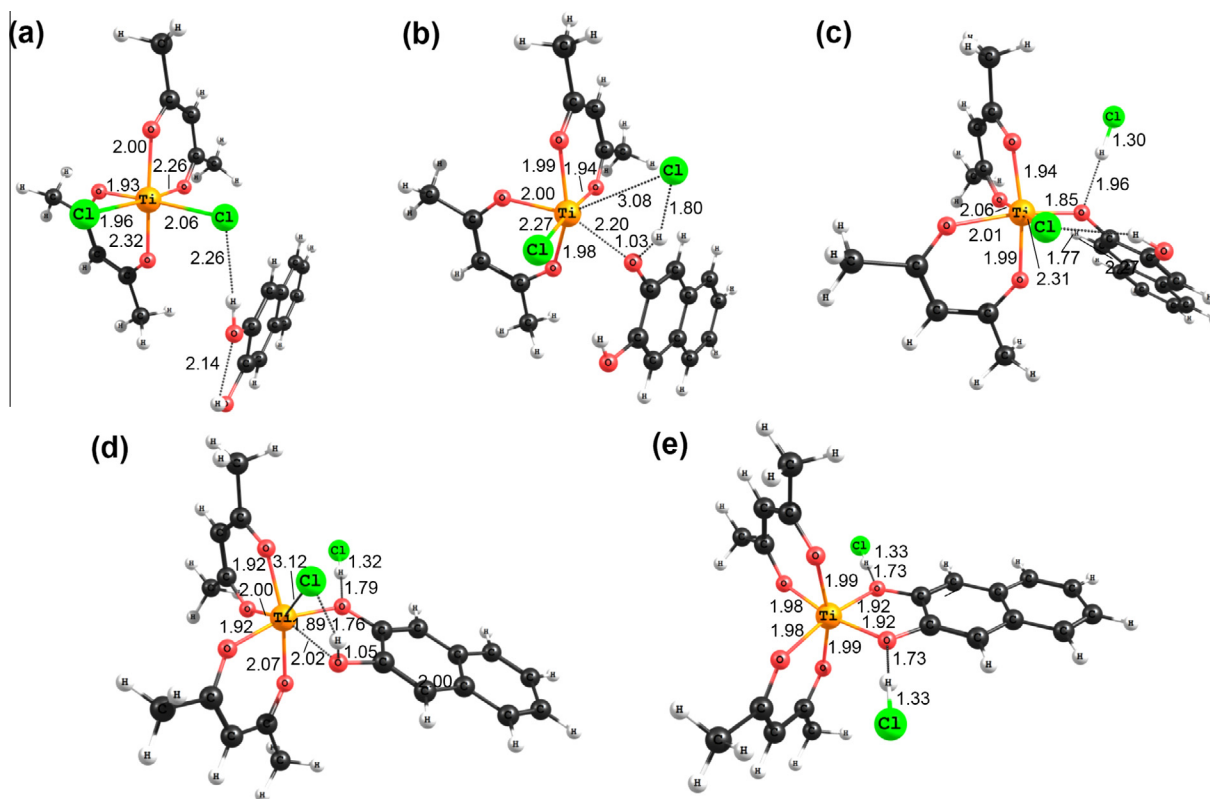


Fig. 7. DFT calculated optimized structures of the $\text{Ti}(\text{acac})_2\text{Cl}_2 + \text{H}_2\text{naph}$ reaction (leading to formation of **3**) with (a) $\text{Reac}_{\text{naph}}$, (b) TS1_{naph} , (c) $\text{Inter}_{\text{naph}}$, (d) TS2_{naph} , and (e) $\text{Prod}_{\text{naph}}$ (bonds breaking or forming are shown with dashed lines in the TS structures).

H_2naph , in contrast to the reaction with biphenol (where the second step was rate-limiting). The product state (Fig. 7e) has a relative Gibbs free energy of $4.1 \text{ kcal mol}^{-1}$ (Table 5). The calculated

near zero relative Gibbs free energies of the intermediate $\text{Inter}_{\text{naph}}$ ($\text{Ti}(\text{CH}_3\text{COCHCOCH}_3)_2(\text{Cl})(\text{Hnaph})$ **7**) and the product $\text{Prod}_{\text{naph}}$ ($\text{Ti}(\text{acac})_2(\text{naph})$ **3**) are in agreement with the experimentally

Table 5
Computed energies for the reaction of $\text{Ti}(\text{acac})_2\text{Cl}_2$ and H_2naph (298.15 K).

$\text{Ti}(\beta)_2\text{Cl}_2$	Computed		
	ΔH (kJ mol ⁻¹)	ΔS (J mol ⁻¹ K ⁻¹)	ΔG (kJ mol ⁻¹)
$\text{ReaC}_{\text{naph}}$	0.0	0.0	0.0
TS1_{naph}	55.8	-62.0	74.2
$\text{Inter}_{\text{naph}}$	1.0	3.8	2.8
TS2_{naph}	52.9	-43.8	66.0
$\text{Prod}_{\text{naph}}$	1.1	-10.0	4.1

found equilibrium between **3** and **7** under second order conditions.

3.4.3. Computational study of the $\text{Ti}(\text{acac})_2\text{Cl}_2 + \text{H}_2\text{mbinaph}$ reaction

We have also performed calculations on the reaction of $\text{Ti}(\text{acac})_2\text{Cl}_2$ with methylenebinaphthol ($\text{H}_2\text{mbinaph}$), which results in formation of product complex **6** containing an 8-membered aryl diolato ring. The chlorine substitution with $\text{H}_2\text{mbinaph}$ occurs as with the substrates H_2biphen and H_2naph , proceeding through two transition states and a 6-coordinated intermediate. (Scheme 3). The optimized geometries for the $\text{H}_2\text{mbinaph}$ reaction are shown in Figure S1 (Supporting Information). The critical distances are similar to the H_2biphen and H_2naph reactions (Figs. 6 and 7). The computed energies (Supporting Information, Table S2) show that the barriers with $\text{H}_2\text{mbinaph}$ are 101.4 kJ mol⁻¹ for the first step and 99.7 kJ mol⁻¹ for the second step (relative to the reactant species). These values are too close to determine which step is rate-limiting for formation of **6**. The computed barriers are also higher than for formation of **4a** and **3** (Tables 4 and 5). The computational results indicate that this is mainly due to a higher enthalpy of activation (compare Table S2 with Tables 4 and 5). The computed activation enthalpies increase from 55.8 kJ mol⁻¹ for H_2naph (formation of **3**) to 65.4 kJ mol⁻¹ for H_2biphen (formation of **4a**) to 89.3 kJ mol⁻¹ for $\text{H}_2\text{mbinaph}$ (formation of **6**). Coordination of the dihydroxyl-substrate to the Ti-complex will result in a strain in the substrate compared to the free (unbound) state; this strain is expected to increase in going from H_2naph to $\text{H}_2\text{mbinaph}$, which can explain the increase in the computed enthalpies.

4. Conclusion

In this paper we have carried out synthetic, kinetic, and computational studies on a series of a remarkably hydrolytically stable bis(acetylacetonato-*O,O'*)(aryl-diolato-*O,O'*)titanium(IV) complexes (**2–6**) containing bidentate ligands (catechol, naphthol, biphenol, binaphthol, or methylenebinaphthol). The aryl-diolato-ligands form 5-, 7- and 8-membered chelating rings. We have also reported the X-ray crystal structure of **7**, corresponding to the mono-chloride intermediate of the substitution reaction resulting in formation of **3**.

The reactivity of $\text{Ti}(\text{RCOCHCOR}')_2\text{Cl}_2$ complexes (**1a–c**) towards chloride substitution according to the β -diketonato ligand ($\text{RCOCHCOR}'^-$) follows the order $(\text{PhCOCHCOPh})^- > (\text{PhCOCHCOCH}_3)^- > (\text{CH}_3\text{COCHCOCH}_3)^-$. This is the same order found experimentally for various transition metal β -diketonato complexes containing the same β -diketonato ligands. The kinetics for the reaction of **1a–c** with biphenol show two kinetically distinct steps, with the second step (which is independent on the concentration of the incoming ligand) being slightly slower than the first. The thermodynamic parameters support an associative or interchange mechanism.

DFT calculations on the reaction of $\text{Ti}(\text{acac})_2\text{Cl}_2$ with different aryl-diolato ligands reveal that chlorine substitution proceeds via a two-step interchange mechanism with the formation of two se-

ven-coordinated transition states and one six-coordinated intermediate. The first reaction step involves the attack of hydroxyl oxygen of the incoming ligand on Ti, dissociation of the chloride ion and proton transfer from the attacking hydroxyl to the chloride. The second reaction step involves attack of the second hydroxyl oxygen on Ti, resulting in displacement of the second chloride ion and ring closure. This step corresponds to an intramolecular reaction, which is in agreement with the experimental kinetics. The computed energies for the formation of **4a** agree remarkably well the experimental thermodynamic values. The proposed interchange mechanism is further supported by the X-ray structure of **7**, which corresponds to the six-coordinated reaction intermediate.

Acknowledgements

Financial assistance by the South African National Research Foundation and the Central Research Fund of the University of the Free State is gratefully acknowledged. This work was supported by the Research Council of Norway through a Centre of Excellence Grant (Grant No. 179568/V30). A grant of computer time from the Norwegian supercomputing program NOTUR (Grant No. NN4654 K) is gratefully acknowledged.

Appendix A. Supplementary data

Supplementary data associated with this article can be found, in the online version, at <http://dx.doi.org/10.1016/j.poly.2013.09.004>.

References

- [1] (a) Y. Qian, J. Huang, M.D. Bala, B. Lian, H. Zhang, H. Zhang, *Chem. Rev.* 103 (2003) 2633;
(b) R. Beckhause, C. Santamaria, *J. Organomet. Chem.* 617 (2001) 81;
(c) E. Manek, D. Hinz, G. Meyer, *Coord. Chem. Rev.* 164 (1997) 5;
(d) J.C. Vites, M.M. Lynam, *Coord. Chem. Rev.* 146 (1995) 1;
(e) J.C. Vites, M.M. Lynam, *Coord. Chem. Rev.* 138 (1995) 71;
(f) R.O. Duthaler, A. Hafner, *Chem. Rev.* 92 (1992) 807;
(g) B.K. Keppler, C. Friese, H.G. Moritz, H. Vongerichten, E. Vogel, *Struct. Bond.* 78 (1991) 98.
- [2] E. Meléndez, *Crit. Rev. Oncol. Hematol.* 42 (2002) 309.
- [3] J.P. Corden, W. Errington, P. Moore, M.G. Partridge, M.G.H. Wallbridge, *J. Chem. Soc., Dalton Trans.* (2004) 1846.
- [4] M. Aizwa, Y. Nosaka, N. Fujii, *J. Non-Cryst. Solids* 128 (1991) 77.
- [5] (a) J. Balsells, T.J. Davis, P. Carroll, P.J. Walsh, *J. Am. Chem. Soc.* 124 (2002) 10336;
(b) A. van der Linden, C.J. Schaverien, N. Meijboom, C. Ganter, A.G. Orpen, *J. Am. Chem. Soc.* 117 (1995) 3008;
(c) T.J. Boyle, N.W. Eilerts, J.A. Heppert, *Organometal* 13 (1994) 2218;
(d) K. Narasaka, *Synthesis* 1 (1991) 1;
(e) K. Mikami, M. Shimizu, *Chem. Rev.* 92 (1992) 1021.
- [6] (a) S.N. Brown, E.T. Chu, M.W. Hull, B.C. Noll, *J. Am. Chem. Soc.* 127 (2005) 16010;
N. Kongprakaiwoot, *Chem. Sci.* 2 (2011) 331.
- [7] B.S. Furniss, A.J. Hannaford, P.W.G. Smith, A.R. Tatchell, *Vogel's Textbook of Practical Organic Chemistry*, fifth ed., John Wiley & Sons, New York, 1994. 409.
- [8] R.C. Fay, R.N. Lowry, *Inorg. Chem.* 6 (1967) 1512.
- [9] N. Serpone, R.C. Fay, *Inorg. Chem.* 6 (1967) 1835.
- [10] T.A. Tsotetsi, A. Kuhn, A. Muller, J. Conradie, *Polyhedron* 28 (2009) 209.
- [11] A. Kuhn, T.A. Tsotetsi, A. Muller, J. Conradie, *Inorg. Chim. Acta* 362 (2009) 3088.
- [12] L. Helm, *MINSQ*, non-linear parameter estimation and model development, least squares parameter optimization, V3.12, MicroMath Scientific Software, Salt Lake City, UT, 1990.
- [13] J.H. Espenson, *Chemical Kinetics and Reaction Mechanisms*, second ed., McGraw-Hill, New York, 1995. 15, 49, 70–75, 156.
- [14] M.J. Frisch, G.W. Trucks, H.B. Schlegel, G.E. Scuseria, M.A. Robb, J.R. Cheeseman, J.A. Montgomery Jr., T. Vreven, K.N. Kudin, J.C. Burant, J.M. Millam, S.S. Iyengar, J. Tomasi, V. Barone, B. Mennucci, M. Cossi, G. Scalmani, N. Rega, G.A. Petersson, H. Nakatsuji, M. Hada, M. Ehara, K. Toyota, R. Fukuda, J. Hasegawa, M. Ishida, T. Nakajima, Y. Honda, O. Kitao, H. Nakai, M. Klene, X. Li, J.E. Knox, H.P. Hratchian, J.B. Cross, V. Bakken, C. Adamo, J. Jaramillo, R. Gomperts, R.E. Stratmann, O. Yazyev, A.J. Austin, R. Cammi, C. Pomelli, J.W. Ochterski, P.Y. Ayala, K. Morokuma, G.A. Voth, P. Salvador, J.J. Dannenberg, V.G. Zakrzewski, S. Dapprich, A.D. Daniels, M.C. Strain, O. Farkas, D.K. Malick, A.D. Rabuck, K. Raghavachari, J.B. Foresman, J.V. Ortiz, Q. Cui, A.G. Baboul, S. Clifford, J. Cioslowski, B.B. Stefanov, G. Liu, A. Liashenko, P. Piskorz, I. Komaromi, R.L. Martin, D.J. Fox, T. Keith, M.A. Al-Laham, C.Y. Peng, A. Nanayakkara, M.

- Challacombe, P.M.W. Gill, B. Johnson, W. Chen, M.W. Wong, C. Gonzalez, J.A. Pople, GAUSSIAN 03, Revision E.01, GAUSSIAN Inc., Wallingford CT, 2004.
- [15] APEX2. (Version 1.0-27), Bruker AXS Inc., Madison, Wisconsin, USA, 2005.
- [16] COSMO. Version 1.48, Bruker AXS Inc., Madison, Wisconsin, USA, 2003.
- [17] SAINT-Plus. Version 7.12 (including XPREF), Bruker AXS Inc., Madison, Wisconsin, USA, 2004.
- [18] SADABS Version 2004/1, Bruker AXS Inc., Madison, Wisconsin, USA, 1998.
- [19] A. Altomare, M.C. Burla, M. Camalli, G.L. Cascarano, C. Giacovazzo, A. Guagliardi, A.G.G. Moliterni, G. Polidori, R. Spagna, *J. Appl. Crystallogr.* 32 (1999) 115.
- [20] L.J. Farrugia, *J. Appl. Crystallogr.* 32 (1999) 837.
- [21] G.M. Sheldrick, SHELXL97 program for crystal structure refinement, University of Göttingen, Göttingen, Germany, 1997.
- [22] International Tables Vol C A.J.C. Wilson (Ed.), International Tables for Crystallography, Volume C, Kluwer Academic Publishers, Dordrecht, The Netherlands, 1995.
- [23] K. Brandenburg, H. Putz, H. Diamond, Release 3.1a, Crystal Impact GbR, Bonn, Germany, 2005.
- [24] G.P. Dahl, B.P. Block, *Inorg. Chem.* 5 (1966) 1394.
- [25] S.N. Brown, E.T. Chu, M.W. Hull, B.C. Noll, *J. Am. Chem. Soc.* 127 (2005) 16010.
- [26] P.V. Rao, C.P. Rao, E.K. Wegelius, E. Kolehmainen, K. Rissanen, *J. Chem. Soc., Dalton Trans.* (1999) 4469.
- [27] B.K. Keppler, M.E. Heim, *Drugs Future* 13 (1988) 637.
- [28] (a) R.C. Fay, N. Serpone, *J. Am. Chem. Soc.* 90 (1968) 5701;
(b) F.A. Cotton, R.H. Holm, *J. Am. Chem. Soc.* 80 (1958) 5658.
- [29] (a) B.K. Keppler, C. Friesen, H.G. Moritz, H. Vongerichten, H. Vogel, *Metal Complexes in Cancer Chemotherapy*, in: B.K. Keppler (Ed.), VCH, Weinheim, Germany, 1993, p. 297;
(b) D.C. Bradley, C.E. Holloway, *J. Chem. Soc. A.* (1969) 282.
- [30] E. Dubler, R. Buschmann, H.W. Schmalle, *J. Inorg. Biochem.* 95 (2003) 97.
- [31] G. Ferguson, C. Glidewell, *Acta Crystallogr., Sect. C: Cryst. Struct. Commun.* 57 (2001) 264.
- [32] L. Matilainen, I. Mutikainen, M. Leskelä, *Acta Chem. Scand.* 50 (1996) 755.
- [33] J. Burgess, S.A. Parsons, *Appl. Organomet. Chem.* 7 (1993) 343.
- [34] F. Basolo, R. Pearson, *Mechanism of Inorganic Reactions*, second ed., John Wiley & Sons, Inc, New York, 1965 (K.F. Purcell, J.C. Kotz, *Inorganic Chemistry*, International Edition; Saunders: London, 1977, pp. 697).
- [35] R.G. Wilkins, *Kinetics and Mechanism of Reactions of Transition Metal Complexes* 2nd thoroughly revised edition, VCH, Weinheim, 1991. pp. 103, 232–242.
- [36] C.A. McAuliffe, D.S. Barratt, *Comprehensive Coordination Chemistry*, in: G. Wilkinson, R.D. Gillard, J.A. McCleverty (Eds.), vol. 3, Pergamon Press, Oxford, 1987, pp. 323–360.
- [37] M. Colapietro, A. Vaciago, D.C. Bradley, M.B. Hursthouse, I.F. Rendall, *J. Chem. Soc., Dalton Trans.* (1972) 1052.
- [38] (a) J.G. Leiboldt, G.J. Lamprecht, E.C. Steinberg, *J. Organometal. Chem.* 397 (1990) 239;
(b) J.G. Leiboldt, S.S. Basson, J.J.J. Schlebush, E.C. Grobler, *Inorg. Chim. Acta* 62 (1982) 113;
(c) J.G. Leiboldt, E.C. Grobler, *Trans. Met. Chem.* 11 (1986) 110;
J.G. Leiboldt, S.S. Basson, *J. Organomet. Chem.* 418 (1991) 113.
- [39] C.J. Cramer, *Essentials of Computational Chemistry: Theories and Models*, second ed., John Wiley & Sons, Inc., New York, 2004.